

## TRANSVERSE SUSCEPTIBILITY OF SINGLE-DOMAIN PARTICLE SYSTEMS

A. Stancu<sup>\*</sup>, L. Spinu<sup>a</sup>

Faculty of Physics, "Al. I. Cuza" University, Iași, 6600, România

<sup>a</sup>AMRI & Physics Dept., University of New Orleans, LA 70148, USA

Simulations of the Transverse Susceptibility (TS) signal for single-domain and for systems of ferromagnetic particles are presented. When calculating the TS for single domains, details are provided concerning the uniaxial and cubic anisotropies. For the uniaxial single-domain particles a 2D critical approach can be used. The TS for cubic anisotropy is essentially a 3D problem that was solved with a micromagnetic Landau-Lifshitz-Gilbert algorithm. Since the TS experimental method is extensively used in the laboratories for the anisotropy evaluation, the importance of this study consists in the fact that it offers a tool for understanding the problems and errors in the correct interpretation of the TS curves.

(Received July 22, 2002; accepted after revision March 12, 2003)

*Keywords:* Magnetic anisotropy, Single-domain particle, Transverse susceptibility

### 1. Introduction

The well-known experimental method of transverse susceptibility (TS) is a method for direct determination of the magnetic anisotropy in particulate magnetic systems. This is due to the fact that, as predicted by Stoner-Wohlfarth model, for non-interacting uniaxial single-domain fine particle systems, the field dependence of transverse susceptibility presents characteristic peaks, located at the anisotropy and switching fields [1]. The conditions, as uniaxial anisotropy, and single-domain non-interacting particles, in which the anisotropy can be determined accurately using this method might appear to be very restrictive. In fact, the same conditions that apply to other usual methods for determining the anisotropy in the case of particulate systems, as single detection point techniques or rotation hysteresis method, are satisfied in many practical cases. For TS experiments an important step in this direction was done by advancing the classical model for TS due to Aharoni [1], by taking into account the influence of the higher order terms of the uniaxial anisotropy [2][3][4][5][6][7], an approach that is important for many usual magnetic uniaxial materials as e.g. cobalt.

In this paper we present the methods used in the TS evaluation for both uniaxial and cubic single-domain particles.

### 2. Transverse susceptibility for single-domain particles

The experimental method of transverse susceptibility (TS) is used for direct measurement of the anisotropy in ferromagnetic systems due to the fact that usually these systems show sharp peaks located at the anisotropy field which makes possible a precise detection and the calculation of these important physical parameters as it was proven for uniaxial single particles within the coherent rotation Stoner-Wohlfarth theory in [1]. The series expansion for the magneto-crystalline uniaxial anisotropy is given by:

---

<sup>\*</sup> Corresponding author: alstancu@uaic.ro

$$W_a = K_1 \sin^2 \theta + K_2 \sin^4 \theta + \dots \quad (1)$$

where  $\theta$  is the angle between the easy axis and the magnetic moment of the particle.

However, this is accurate only when the angle between the easy axis and the magnetic moment is sufficiently small. In the TS experiment, it was shown that the particles with the easy axis oriented near  $90^\circ$  to the DC field direction are responsible for the peaks located at  $\pm H_K$ , where  $H_K = [2|K_1|/(\mu_0 M)]$  is the anisotropy field. The shape of the TS curve is significantly influenced by the particles with the easy axis oriented near  $90^\circ$ . For these particles, when the field is near  $H_K$  the angle between their easy axis and the magnetic moment is close to  $90^\circ$ . Therefore, neglecting the higher order terms in the TS calculation is a major source of errors. For materials with high values of  $K_2$  this error is more significant.

In the TS experiment one applies to the sample a system of two magnetic fields (see Fig. 1), one DC field that is considered on the Oz direction, and a small amplitude AC field, on the Ox direction in Fig. 1. The material easy axis (EA) orientation is given by the spherical angles  $(\theta_a, \varphi_a)$  and, if one can define a single orientation of the sample magnetization, as in the coherent rotation model, the orientation of the magnetic moment is given by the radial unit vector in the spherical coordinates system  $(\vec{u}_R, \vec{u}_\theta, \vec{u}_\varphi)$ . The angle between the total applied field and the Oz axis at a certain moment is  $\theta_h$ . In the TS experiment, one measures the limit:

$$\chi_t = \lim_{\theta_h \rightarrow 0} \frac{dM_x}{dH_x} \quad (2)$$

that will be referred to as the transverse susceptibility in the experimental setup described in Fig. 1.

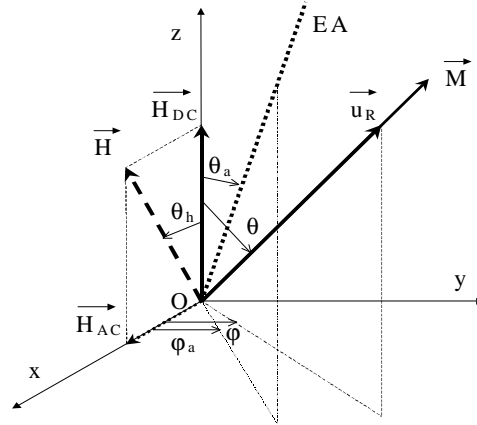


Fig. 1. Transverse susceptibility experiment for an uniaxial single-domain ferromagnetic particle.

When a similar methodology with that in [1] is applied we have found the expression for the TS when the second term in the series expansion of the anisotropy free energy is also taken into account [2]:

$$\chi_T = \frac{3}{2} \chi_0 \left\{ \cos^2 \varphi_a \frac{\cos^2 \theta}{h_{DC} \cos \theta + \cos(2\Delta\theta) + k_2 [\cos(2\Delta\theta) - \cos(4\Delta\theta)]} - \sin^2 \varphi_a \frac{\sin(\Delta\theta)}{h_{DC} \sin \theta} \right\} \quad (3)$$

where  $h_{DC} = H_{DC}/[2|K_1|/(\mu_0 M)]$  is the reduced DC field,  $k_2 = K_2/|K_1|$ ,  $\Delta\theta = \theta - \theta_a$ ,  $\chi_0 = (\mu_0 M)^2/3|K_1|$  and  $M$  is the saturation magnetization of the particle.

## 2.1 Critical curve approach for the uniaxial case

The TS evaluation is simpler for  $k_2 = 0$  due to the fact that the free energy has only two minima which can be selected with the well-known SW astroid critical curve. When  $k_2 \neq 0$ , the free energy landscape is more complicated. The number of minima is higher and the selection of the stable state in the TS measurement is more complex and the use of the critical curves formalism in this case is a helpful tool. Using the same strategy as Thiaville in [8] and [9], one expresses the normalized free energy density as:

$$w = w_a - 2\vec{h}_0 \cdot \vec{u}_M \quad (4)$$

where  $w_a$  is the normalized anisotropy free energy,  $h_0 = H/[2|K_1|/(\mu_0 M)]$ ,  $H$  is the applied field, and the orientation of the magnetization is given by the unit vector  $\vec{u}_M$ . For a system with uniaxial anisotropy (easy axis) the applied field direction and the magnetic moment direction are in the same plane. Thus, one can choose the Oz axis direction on the easy axis and one can solve a 2D problem instead of the initial 3D problem. In spherical coordinates, the anisotropy free energy density can be expressed as a function of the  $\theta$  angle only, and  $\vec{u}_M = \vec{u}_R$ . The equilibrium and stability conditions are given by:

$$\begin{cases} \frac{dw}{d\theta} = \frac{dw_a}{d\theta} - 2\vec{h}_0 \cdot \vec{u}_\theta = 0 & (\text{equilibrium condition}) \\ \frac{d^2w}{d\theta^2} = \frac{d^2w_a}{d\theta^2} + 2\vec{h}_0 \cdot \vec{u}_R > 0 & (\text{stability condition}) \end{cases} \quad (5)$$

where the following relations have been used:

$$\begin{cases} \vec{u}_R = -\frac{d\vec{u}_\theta}{d\theta} \\ \vec{u}_\theta = \frac{d\vec{u}_R}{d\theta} \end{cases} \quad (6)$$

Replacing the inequality sign with equal in the stability condition, one obtains the condition for the critical field that separates the stable from the unstable regime. The critical field vector,  $\vec{h}_{0c}$  is defined by both equilibrium and critical stability conditions:

$$\begin{cases} \frac{dw_a}{d\theta} - 2\vec{h}_{0c} \cdot \vec{u}_\theta = 0 & (\text{equilibrium condition}) \\ \frac{d^2w_a}{d\theta^2} + 2\vec{h}_{0c} \cdot \vec{u}_R = 0 & (\text{critical stability condition}) \end{cases} \quad (7)$$

In fact, the first equation gives the  $\theta$  component of the critical field vector and the second the radial component. The equilibrium equation in (7) represents in the plane a line perpendicular to the vector  $\vec{u}_\theta$ , that is parallel to  $\vec{u}_R$ , and the critical stability equation is a line perpendicular to  $\vec{u}_R$ , which is parallel to  $\vec{u}_\theta$ . The tip of the critical field vector is at the intersection of these two lines (see Fig. 2). Taking into account this feature, the critical field vector can be written as:

$$\begin{aligned} \vec{h}_{0c} &= \frac{1}{2} \frac{dw_a}{d\theta} \vec{u}_\theta - \frac{1}{2} \frac{d^2w_a}{d\theta^2} \vec{u}_R = \\ &= -\frac{1}{2} \left( \frac{dw_a}{d\theta} \sin \theta + \frac{d^2w_a}{d\theta^2} \cos \theta \right) \vec{u}_1 + \frac{1}{2} \left( \frac{dw_a}{d\theta} \cos \theta - \frac{d^2w_a}{d\theta^2} \sin \theta \right) \vec{u}_2 \end{aligned} \quad (8)$$

where  $(\vec{u}_1, \vec{u}_2)$  are the unit vectors in the Cartesian coordinates associated to the same 2D region.

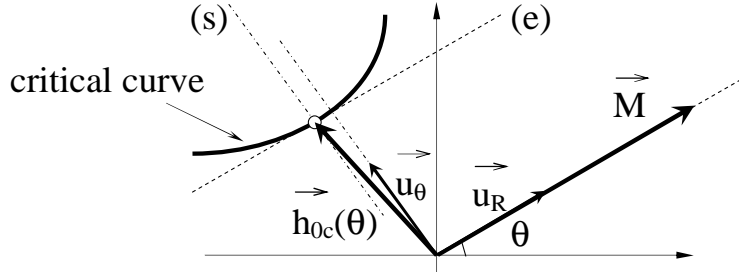


Fig. 2. Critical curve, critical field vector, the equilibrium line (e) and the critical stability line (s).

The tip of the critical field vector,  $\vec{h}_{0c}(\theta)$ , gives the critical curve for a certain expression of the anisotropy free energy density, which is in agreement with the assumption that the 2D calculus is allowed. The derivative of the critical field vector with respect to the angle  $\theta$  gives the direction of the tangent direction to the critical curve. Using (6) in the calculus of this derivative one obtains the expression:

$$\frac{d\vec{h}_{0c}}{d\theta} = -\frac{1}{2} \frac{d}{d\theta} \left( w_a + \frac{d^2 w_a}{d\theta^2} \right) \vec{u}_R \quad (9)$$

We observe that, for a given value of the angle  $\theta$ , the tangent to the critical curve is parallel to the direction of the equilibrium orientation of the magnetization given by  $\vec{u}_R$ . The critical curve has a cusp when the absolute value of the critical field vector has a extremum value. So, using (9), the zeros of the equation:

$$\frac{d}{d\theta} \left( w_a + \frac{d^2 w_a}{d\theta^2} \right) = 0 \quad (10)$$

give the  $\theta$  angles for which a cusp appears on the critical curve. Since the derivative of the critical field vector with respect to the  $\theta$  angle in cusps is zero (see (9)), and the derivatives signs are opposite before and after the cusp, one may also say that the critical curve sense, given by the orientation of the derivative of the critical field vector, is also changing in the cusps. To see how these rules are working, one can check them on the most simple case, the particle with uniaxial anisotropy, when is taken into account only the first term in the series expansion of the anisotropy free energy density, which corresponds to the case  $k_2 = 0$ . In this case, the anisotropy free energy is given by:

$$w_a = \sin^2 \theta \quad (11)$$

and

$$\begin{cases} \frac{dw_a}{d\theta} = \sin(2\theta) \\ \frac{d^2 w_a}{d\theta^2} = 2 \cos(2\theta) \end{cases} \quad (12)$$

Using (12) in (8) and (9), one obtains the expression of the critical field vector:

$$\vec{h}_{0c}(\theta) = -\vec{u}_1 \cos^3 \theta + \vec{u}_2 \sin^3 \theta \quad (13)$$

and for the critical field vector derivative

$$\frac{d\vec{h}_{0c}}{d\theta} = 3\vec{u}_R \sin \theta \cos \theta \quad (14)$$

The expression of the critical field vector, (13), is the parametric formulation of the well-known astroid curve and the derivative (14) is showing that on the curve there are four cusps, for  $\theta = 0, \pi/2, \pi$  and  $3\pi/2$ , as presented on Fig. 3.

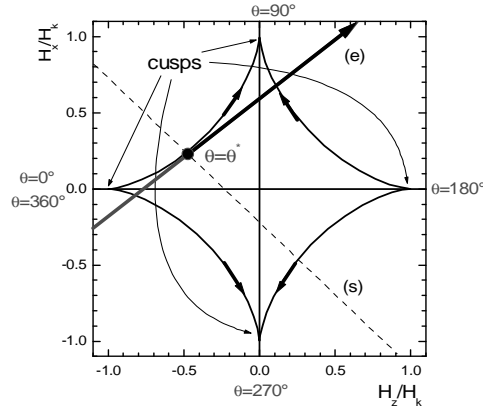


Fig. 3. Critical curve for the uniaxial anisotropy,  $k_2 = 0$ .

When  $k_2$  is not zero, the anisotropy free energy density is given by:

$$w_a = \sin^2 \theta + k_2 \sin^4 \theta \quad (15)$$

the derivatives are:

$$\begin{cases} \frac{dw_a}{d\theta} = 2 \sin \theta \cos \theta + 4k_2 \sin^3 \theta \cos \theta \\ \frac{d^2 w_a}{d\theta^2} = 2(1 - 2 \sin^2 \theta) + 4k_2 \sin^2 \theta (3 - 4 \sin^2 \theta) \end{cases} \quad (16)$$

the critical field vector is:

$$\begin{aligned} \vec{h}_{0c}(\theta) = & -\vec{u}_1 \cos^3 \theta (1 + 6k_2 \sin^2 \theta) + \\ & + \vec{u}_2 \sin^3 \theta (1 - 4k_2 + 6k_2 \sin^2 \theta) \end{aligned} \quad (17)$$

and the derivative of the critical field vector is:

$$\frac{d\vec{h}_{0c}}{d\theta} = 3\vec{u}_R \sin \theta \cos \theta (1 - 4k_2 + 10k_2 \sin^2 \theta) \quad (18)$$

From (18) one can see that supplementary cusps are obtained in comparison with the ones observed in the  $k_2 = 0$  case, only if the equation

$$1 - 4k_2 + 10k_2 \sin^2 \theta = 0 \quad (19)$$

has a solution, that is, if the square of the sinus from  $\theta$  is in the interval  $[0,1]$ , which condition is equivalent with:

$$0 \leq \frac{4k_2 - 1}{10k_2} \leq 1 \quad (20)$$

If  $k_2 \in (-1/6, 1/4)$  the critical curve has no supplementary cusp. It can be shown that in the case of  $k_2$  values bigger than  $(1/4)$ , supplementary pairs of cusps do appear for  $\theta = 0$  and  $\pi$ . For values smaller than  $-1/6$  such pair of cusps are appearing in  $\theta = \pi/2$  and  $3\pi/2$ .

To calculate the TS using the critical curves previously calculated it is essential to find the stable equilibrium state of the magnetic moment at a certain moment from these curves. In fact, the critical curve can provide an interval of values for the  $\theta$  angle in which there is only one solution. This is quite simple when  $k_2 \in (-1/6, 1/4)$  and the critical curve has only four cusps, but it is not so obvious in the cases with eight cusps. In the first case inside the critical curve, in each point, there are possible two stable equilibrium states and one of unstable equilibrium. One can say that there are two energy minima separated by a minimum. Out of the critical curve, in the same case, only one minimum is possible. The eight-cusps systems have inside the critical curve regions with more than two minima which gives the difficulty in choosing the right one, followed by the magnetic moment in its dynamic.

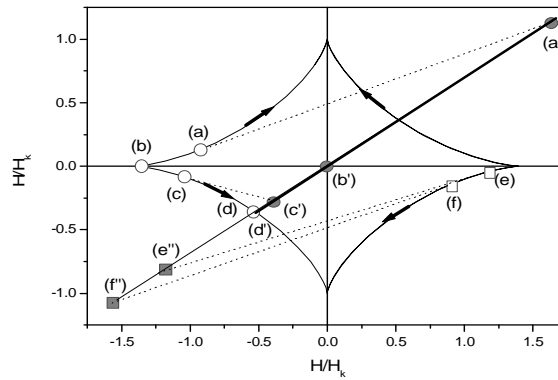


Fig. 4. The stable equilibrium orientation of the magnetization vector ( $k_2 = 0.2$ ).

In Fig. 4 one presents the stable equilibrium states for a uniaxial anisotropy single-domain particle with  $k_2 = 0.2$ . The external field (which in the TS experiment is the DC field) is applied on the direction  $(a'b'c'd'e''f'')$  decreasing from  $(a')$  to  $(f'')$ . One observes that the tangents from the critical curves corresponding to stable equilibrium orientations of the magnetization vector are starting for the fields  $(a', b', c', d')$  from the region  $(abcd)$  on the critical curve. When the applied field passes in the region  $(d', e'', f'')$  the stable equilibrium states are associated to tangents started from the  $(ef)$  region.

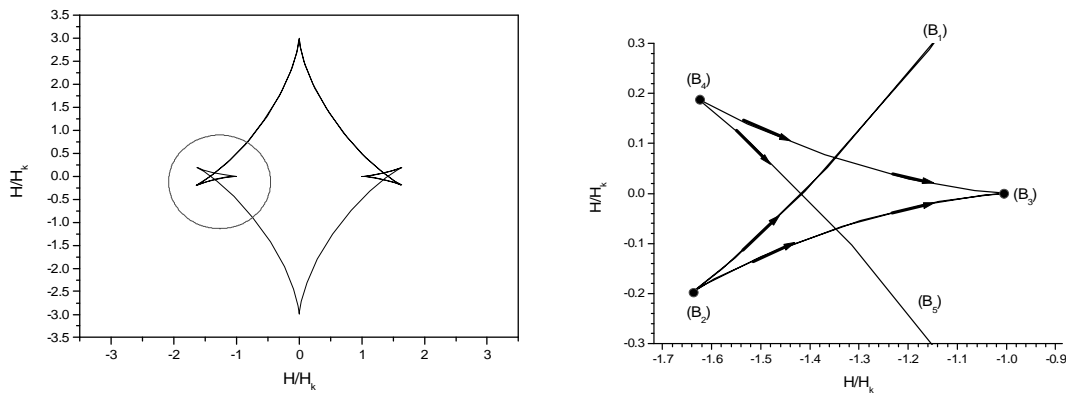


Fig. 5. (left) The critical curve for  $k_2 = 1.0$ ; (right) Detail of the region marked on the left figure.

In Fig. 5 one presents the critical curve for  $k_2 = 1.0$ . It can be easily observed that the cusp characterized by  $\theta = 0$  (point b on the critical curve shown in Fig. 4) is in this case transformed in three cusps. The critical curve follows the path  $(B_1, B_2, B_3, B_4, B_5)$  where  $B_2, B_3$  and  $B_4$  are the cusp points. The cusp  $B_3$  is now the one for  $\theta = 0$ . As shown in [8] it can be found a rule that can be applied even in these cases to find the stable equilibrium orientation for the system.

A systematic analysis have shown that the critical curve approach can be applied for the 2D case quite efficiently. We have compared the results obtained with this method with the micromagnetic method, that is presented below, and a good agreement was found in each case. However, even in the case of uniaxial anisotropy there are cases in which the bi-dimensional image is not sufficient. For example, uniaxial systems  $K_1 < 0$ , for different values of the  $k_2$  parameter corresponds to systems with the easy axes forming a cone (an easy cone). In these cases one observe in certain conditions jumps from one cusp point to another. This is due to the fact that the magnetic moment can move freely around the easy cone surface. Especially due to these cases, the critical curve approach has a limited value in the calculation of the TS curves. For cubic anisotropy, the 2D critical curve can not be used anymore because the applied field direction, the easy axis direction and the magnetization direction aren't in the same plane. The cubic anisotropy case is essentially a 3D problem that needs a full 3D approach. The complexity of the critical approach presented in [9] and [10] is an argument in the favor of the micromagnetic method that will be presented in the next section.

## 2.2 Micromagnetic algorithm

The micromagnetic model used is based on the Landau-Lifshitz-Gilbert equation[11].

The dynamics of the magnetization vector  $\vec{M}$  of each particle in the applied field  $\vec{H}$  is described by the Landau-Lifshitz-Gilbert (LLG) equation [11]:

$$\frac{d\vec{M}}{dt} = -|\gamma|(\vec{M} \times \vec{H}) + \frac{\alpha}{|\vec{M}|} \left[ \vec{M} \times \left( \frac{d\vec{M}}{dt} \right) \right] \quad (21)$$

where  $M = |\vec{M}|$  is assumed to be invariable,  $\alpha$  is the phenomenological damping constant assumed to be positive and  $\gamma$  is the gyromagnetic factor. With the following notations:

$$\vec{h} = \frac{\vec{H}}{M}, \tau = \frac{t\gamma M}{1 + \alpha^2} \quad (22)$$

and using spherical co-ordinates, equation (21) can be written as:

$$\begin{cases} \frac{d\theta}{d\tau} = h_\varphi + \alpha h_\theta \\ \frac{d\varphi}{d\tau} = \frac{-h_\theta + \alpha h_\varphi}{\sin \theta} \end{cases} \quad (23)$$

with

$$\begin{cases} h_\theta = h_{a\theta} + h_{o\theta} \\ h_\varphi = h_{a\varphi} + h_{o\varphi} \end{cases} \quad (24)$$

and

$$\begin{cases} h_{a\theta} = \frac{1}{M} \left( \frac{2|K_1|}{\mu_0 M} \right) \left( -\frac{1}{2} \frac{\partial w_a}{\partial \theta} \right) \\ h_{a\varphi} = \frac{1}{M} \left( \frac{2|K_1|}{\mu_0 M} \right) \left( -\frac{1}{2 \sin \theta} \frac{\partial w_a}{\partial \varphi} \right) \end{cases} \quad (25)$$

named equivalent anisotropy fields, where  $w_a$  is the anisotropy free energy density.

### Uniaxial anisotropy

For uniaxial anisotropy, if the easy axis orientation is given by the unit vector  $\vec{u}_a$ , and the orientation of the magnetization vector is on the direction of the  $\vec{u}_R$  unit vector (in spherical coordinates), the anisotropy free energy can be expressed as:

$$w_a = \text{sgn}(K_1) \times \left[ 1 - (\vec{u}_a \cdot \vec{u}_R)^2 \right] + k_2 \left[ 1 - (\vec{u}_a \cdot \vec{u}_R)^2 \right]^2 \quad (26)$$

and the equivalent anisotropy fields are given by:

$$\begin{cases} h_{a\theta} = \frac{1}{M} \left( \frac{2|K_1|}{\mu_0 M} \right) (\vec{u}_a \cdot \vec{u}_R) (\vec{u}_a \cdot \vec{u}_\theta) \left\{ \text{sgn}(K_1) + 2k_2 \left[ 1 - (\vec{u}_a \cdot \vec{u}_R)^2 \right] \right\} \\ h_{a\varphi} = \frac{1}{M} \left( \frac{2|K_1|}{\mu_0 M} \right) (\vec{u}_a \cdot \vec{u}_R) (\vec{u}_a \cdot \vec{u}_\varphi) \left\{ \text{sgn}(K_1) + 2k_2 \left[ 1 - (\vec{u}_a \cdot \vec{u}_R)^2 \right] \right\}. \end{cases} \quad (27)$$

### Cubic anisotropy

For cubic anisotropy, the anisotropy free energy density can be expressed as a function of the relative orientation of the [100], [010] and [001] axes with respect to the magnetization vector. If one uses the Euler angles to define the orientation of these axes  $(\varphi_a, \theta_a, \psi_a)$ , one obtains,

$$\begin{cases} \vec{u}_{[100]} = +\cos\psi_a (\vec{u}_1 \cos\varphi_a + \vec{u}_2 \sin\varphi_a) + \sin\psi_a (-\vec{u}_1 \sin\varphi_a \cos\theta_a + \vec{u}_2 \cos\varphi_a \cos\theta_a + \vec{u}_3 \sin\theta_a) \\ \vec{u}_{[010]} = -\sin\psi_a (\vec{u}_1 \cos\varphi_a + \vec{u}_2 \sin\varphi_a) + \cos\psi_a (-\vec{u}_1 \sin\varphi_a \cos\theta_a + \vec{u}_2 \cos\varphi_a \cos\theta_a + \vec{u}_3 \sin\theta_a) \\ \vec{u}_{[001]} = \vec{u}_1 \sin\varphi_a \sin\theta_a - \vec{u}_2 \cos\varphi_a \sin\theta_a + \vec{u}_3 \cos\theta_a \end{cases} \quad (28)$$

where  $(\vec{u}_1, \vec{u}_2, \vec{u}_3)$  are the unit vectors of the Cartesian coordinates of the laboratory system. The free energy density in these conditions is given by:

$$\begin{aligned} w_a = \text{sgn}(K_1) \times & \left[ (\vec{u}_{[100]} \cdot \vec{u}_R)^2 (\vec{u}_{[010]} \cdot \vec{u}_R)^2 + (\vec{u}_{[010]} \cdot \vec{u}_R)^2 (\vec{u}_{[001]} \cdot \vec{u}_R)^2 + (\vec{u}_{[001]} \cdot \vec{u}_R)^2 (\vec{u}_{[100]} \cdot \vec{u}_R)^2 \right] + \\ & + k_2 (\vec{u}_{[100]} \cdot \vec{u}_R)^2 (\vec{u}_{[010]} \cdot \vec{u}_R)^2 (\vec{u}_{[001]} \cdot \vec{u}_R)^2 \end{aligned} \quad (29)$$

Using (29) in (25) one obtains the equivalent anisotropy fields.

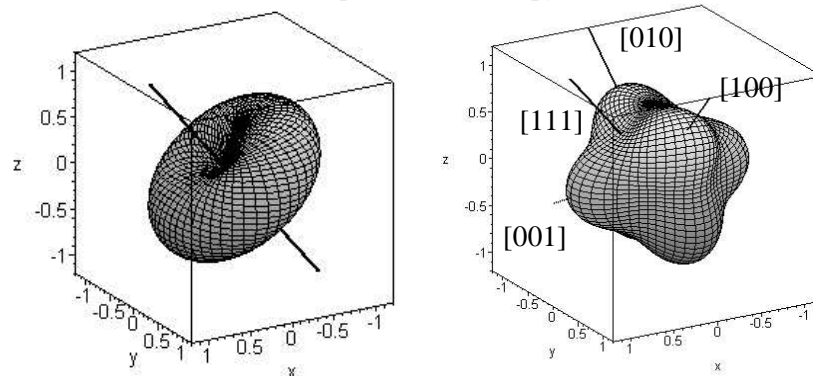


Fig. 6. The free energy surfaces for uniaxial (left) and cubic (right) anisotropies.

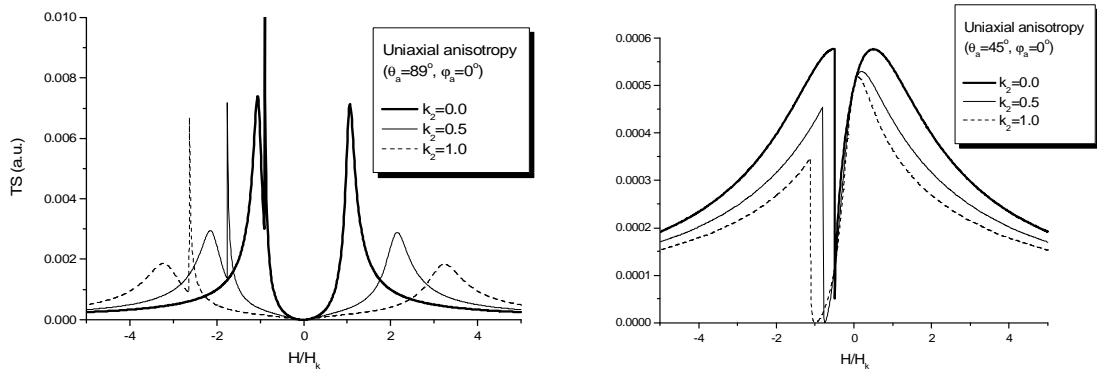


The TS process was simulated by a sequence of fields, identical to those applied in the experiment. At each step, the LLG equation is integrated until the motion of the magnetic moments can be neglected.

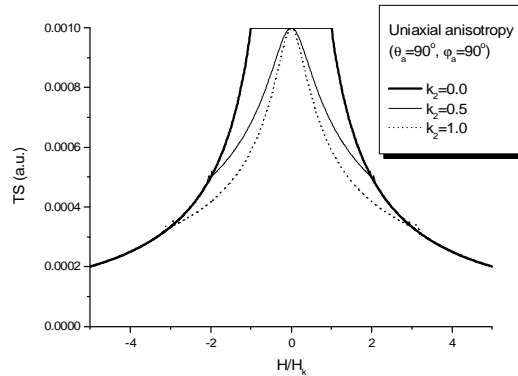
### 3. Simulates TS curves

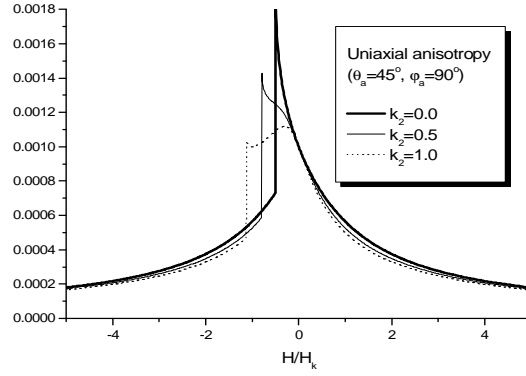
In Figs. 7-11 one show results obtained with the LLG algorithm for single-domain and for systems of particles. In Figs. 7-8 the TS curves are for uniaxial single-domain particles and in Figs. 9-10 for cubic anisotropy with  $K_1 = -5.0 \cdot 10^{-3} \text{ J/m}^3$ ,  $k_2 = -0.5$  (Nickel). One observes that the differences between the uniaxial and cubic anisotropies are increasingly significant with the angle between the [111] axis and the applied DC field. This is quite understandable if one takes into account the differences of the free energy surface in the two cases. One can mention that in order to systematically study the TS of a single-domain ferromagnetic particle with cubic anisotropy, the number of distinct situations is much higher that in the uniaxial case. Due to the possibility to use the critical curve approach, the uniaxial case is a very important tool for testing the micromagnetic model. However, our analyses have shown that in certain cases the sensitivity of the micromagnetic algorithm to factors like the AC field amplitude, is much higher that usual. The discussion of these cases is out of the objectives of this paper.

For an assembly of non-interacting single domain particles the TS response is given by the integral of the transverse susceptibility of each particle over the easy axis distribution. Fig. 11 displays the results obtained for a randomly oriented system for different values of the second order anisotropy parameter,  $k_2$ . The effect of  $k_2$  on the TS curve of the ensemble can be observed especially on the peaks position. The other parameters, like the orientation distribution, influence the shape of the TS curve.

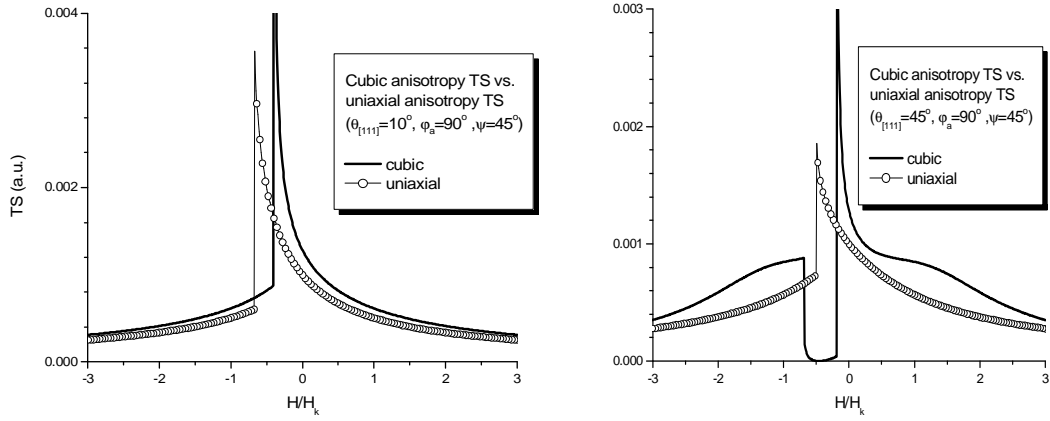


Figs. 7. TS signal when  $\theta_a = 89^\circ$ ,  $\phi_a = 0^\circ$  (left) and  $\theta_a = 45^\circ$ ,  $\phi_a = 0^\circ$  (right) for a uniaxial single-domain particle.



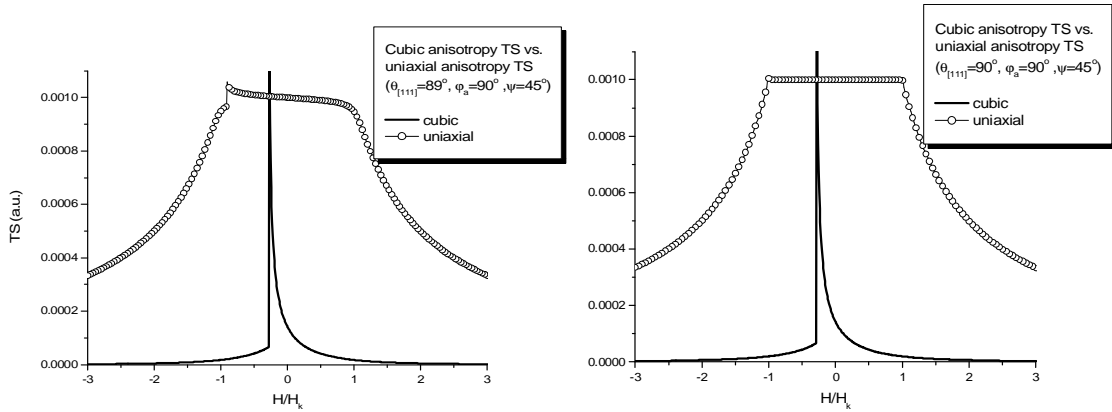


Figs. 8. TS signal when  $\theta_a=90^\circ$ ,  $\varphi_a=90^\circ$  (left) and  $\theta_a=45^\circ$ ,  $\varphi_a=90^\circ$  (right) for a uniaxial single-domain particle.



Figs. 9. Comparison between TS signal for cubic and uniaxial single-domain particles:

$\theta_{[111]} = 10^\circ$ ,  $\varphi_a = 90^\circ$  (left) and  $\theta_{[111]} = 45^\circ$ ,  $\varphi_a = 90^\circ$  (right).



Figs. 10. Comparison between TS signal for cubic and uniaxial single-domain particles:

$\theta_{[111]} = 89^\circ$ ,  $\varphi_a = 90^\circ$  (left) and  $\theta_{[111]} = 90^\circ$ ,  $\varphi_a = 90^\circ$  (right).

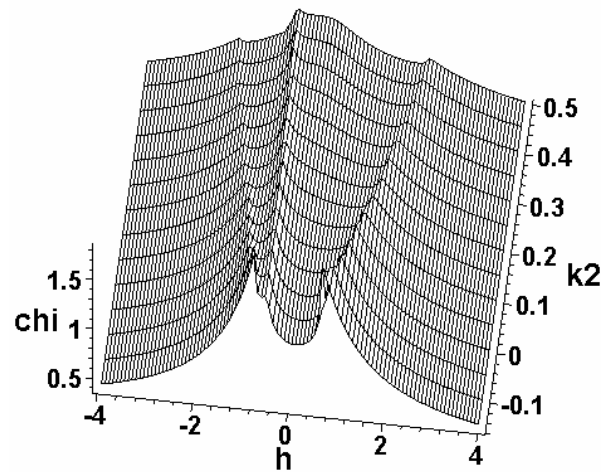


Fig. 11. The TS signal for a system of non-interacting, randomly oriented uniaxial particles.

## 5. Conclusions

In this paper we have presented a systematic illustration of the micromagnetic calculation of the TS for uniaxial and cubic single-domain particles. The results are important for understanding the shape of the TS signal for systems of single-domain particles distributed as a function of orientation.

## References

- [1] A. Aharoni, E. M. Frei, S. Shtrikman, D. Treves, *Bull. Res. Council. Isr.* **6A**, 215 (1957).
- [2] L. Spinu, Al. Stancu, H. Srikanth, C. J. O'Connor, *Appl. Phys. Lett.* **80**, 276 (2002).
- [3] Al. Stancu, L. Spinu, C. J. O'Connor, *J. Magn. Magn. Mater.* **242-245**(2), 1026 (2002).
- [4] L. Spinu, Al. Stancu, H. Srikanth, C. J. O'Connor, *Physica B* **306/1-4**, 221 (2001).
- [5] L. Spinu, Al. Stancu, L. D. Tung, J. Fang, P. Postolache, H. Srikanth, C. J. O'Connor, *J. Magn. Magn. Mater.* **242-245**(2), 604 (2002).
- [6] L. Spinu, L. D. Tung, V. Kolesnichenko, J. Fang, A. Stancu, C. J. O'Connor, INTERMAG 2002, paper FC07.
- [7] L. Spinu, A. Stancu, L. D. Tung, P. Postolache, J. Fang, C. J. O'Connor, MMM Conference, Seattle 2001.
- [8] A. Thiaville, *J. Magn. Magn. Mater.* **182**, 5 (1998).
- [9] A. Thiaville, *Phys. Rev. B* **61**(18), 12221 (2000).
- [10] C. R. Chang, *J. Appl. Phys.* **69**(4), 2431 (1991).
- [11] P. R. Gillete, K. Oshima, *J. Appl. Phys.* **29**, 529 (1958).